

The Fluorescence Detector of the Pierre Auger Observatory

Petr Nečesal for the Pierre Auger Collaboration

Fyzikální ústav AV ČR, v. v. i., Na Slovance 2, Praha 8, 182 21, Czech Republic and
 Observatorio Pierre Auger, Av. San Martín Norte 304, 5613 Malargüe, Argentina;
http://www.auger.org/archive/authors_2010_08.html

E-mail: necosal@fzu.cz

Abstract. The Pierre Auger Observatory is a facility designed for the study of ultra-high energy cosmic rays. The Observatory combines two different types of detectors: a surface array of 1600 water Cherenkov stations placed on a 1.5 km triangular grid covering over 3000 km²; and a fluorescence detector of 24 telescopes located in 4 buildings at the perimeter of the surface array. The fluorescence telescopes, each consisting of 440 photomultipliers, collect the ultraviolet light produced when the charged secondary particles in an air shower excite nitrogen molecules in the atmosphere. Because the intensity of the nitrogen fluorescence is proportional to the energy deposited in the atmosphere during the air shower, the air fluorescence measurements can be used to make a calorimetric measurement of the cosmic ray primary energy. Showers observed independently by the surface array and fluorescence telescopes, called hybrid events, are critical to the function of the Observatory, as they allow for a model-independent calibration of the surface detector. In this paper I describe the detector and the most important measurements.

1. Introduction

Ultra-high energy cosmic rays (UHECRs) are particles coming to the atmosphere of the Earth with energies that can exceed 10²⁰ eV. While the first observation of cosmic rays (CRs) was made one hundred years ago, origins of these particles is not yet understood. Much of the reason is because of the very low flux of UHECRs at Earth. The differential flux of UHECRs is steeply falling with energy, and can be described by a power law

$$\frac{dN}{dE} \propto E^{-\gamma} \quad (1)$$

with spectral index γ between 2.6 and 3.2. One can find two significant points in the energy spectrum – at 4×10^{15} eV there is so called 'knee' where γ changes from 2.7 to 3.1 [1] and known 'ankle' can be found at 4×10^{18} eV with another spectral index change from 3.3 to 2.6 [2]. Processes and mechanisms of achieving ultra-high energies are still undiscovered. So the main questions which people want to answer concern composition, energy spectrum and sources of UHECRs.

Primary CRs hitting the Earth's atmosphere interact with air molecules and fragment. The secondary particles produced in this collision will undergo further hadronic and electromagnetic interactions, ultimately producing an extensive air shower cascade. As the air shower develops in the atmosphere the number of secondary particles increases and their average energy falls.

Due to energy losses and decays, the shower will reach a maximum size, and then number of particles in the shower will begin to decrease. However, there are still enough energetic particles in a vertical air shower which can hit ground and can be detected by ground detectors. With increasing zenith angle of the primary particle an air shower must propagate through larger atmospheric mass and therefore only less particles survive at the ground level.

There are two possible types of UHECR detection – direct and indirect methods. Direct methods can be performed by means of satellites and balloons, but cannot considerably measure UHECR at energies larger than 10^{14-15} eV because of small statistics (Eq. 1). On the other hand indirect methods require sufficient energy ($E \gtrsim 10^{15}$ eV) to develop shower and large detector area is necessary. Indirect methods are based on the measurement of secondary particles that reach the ground in array of Cherenkov detectors, scintillators or muon detectors or on the collection of the isotropic fluorescence light. Secondary charged particles in the shower excite nitrogen molecules, which then isotropically emit fluorescence light into several bands between 300 and 420 nm. These photons can be detected by fluorescence telescopes.

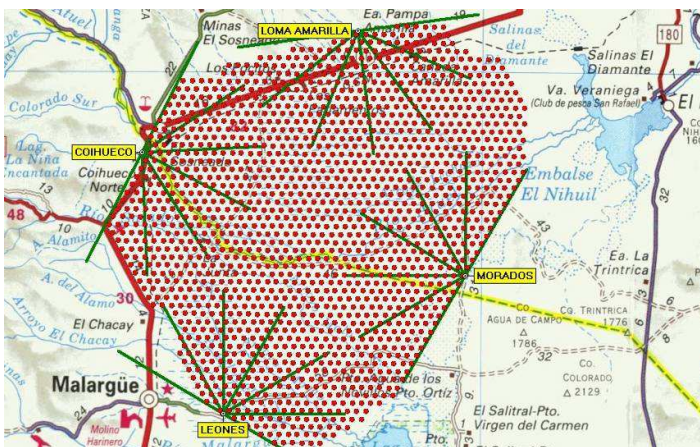


Figure 1. The detector layout of the Pierre Auger Observatory. Red dots indicate SD stations which are overviewed by 4 FD buildings. There are 6 fluorescence telescopes in each building. Green lines indicate field of view of each telescope.



Figure 2. A picture of an SD station and FD building. Each station has its own solar panel with battery and communication antenna. There is also the antenna nearby the FD building.

2. Pierre Auger Observatory

The Pierre Auger Observatory [3] is a facility studying UHECRs by means of two type of detectors: a surface detector (SD) which is composed of 1600 water Cherenkov stations and a fluorescence detector (FD) that comprises 24 fluorescence telescopes. The southern site of the Observatory is located in province Mendoza in Argentina near the city Malargüe (69° W, 35° S, 1420 m a.s.l.), the northern site is intended to be built in Colorado, USA. The layout of the southern site detectors is shown in Fig. 1, and the picture of an SD station and an FD building is shown in Fig. 2. Stations are deployed on a triangular grid with 1.5 km spacing. They cover an area of over 3000 km² and they have nearly 100 % duty cycle. There are 3 photomultipliers in pure water in each station.

The Pierre Auger Observatory is designed to measure UHECRs with energy above $\sim 10^{18}$ eV. However, there is also a low energy extension of SD station infill with plastic scintillators beneath the stations to detect muons (AMIGA [4]) and a set of 3 fluorescence telescopes with high

elevation called HEAT [4]. An extensive program of atmospheric monitoring is essential part of the Observatory not only to control uncertainties concerning FD.

3. Fluorescence Detector

There are 4 buildings with 6 fluorescence telescopes each that overlook the area of SD stations (Fig. 1). Each telescope uses Schmidt optics and consists of a wide-angle, segmented spherical mirror, a spherical focal plane, a UV 300-410 nm passband filter, and a refractive corrector ring at the aperture of the telescope. The telescope field of view is 30° (in azimuth) \times 28° (in elevation) so each building has 180° azimuth range (the 3 high-elevation telescopes observe 30° to 60° in elevation). There are 440 photomultipliers in the focal plane which collect reflected light. The longitudinal profile of a shower is thus measured as an image of active PMT pixels along the shower axis. The layout of the FD geometry is shown in Fig. 3.

There are several trigger levels. The first level digitizes signals from an analog board in each pixel at 10 MHz. The second level trigger is also an internal trigger to search for track segments of at least five active pixels. Every 100 ns, a scan over the full camera is performed and the triggered pixels are searched for track-like patterns. The third level trigger is a software algorithm that rejects events caused by lightning, muons which impact the focal plane, or randomly triggered pixels.

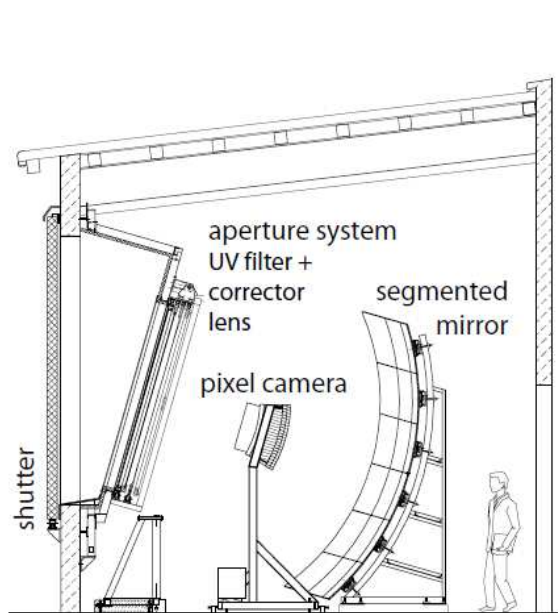


Figure 3. A scheme of telescope geometry. Light comes through the aperture, covered by a UV filter and a corrector ring, and it is reflected by a segmented mirror to the pixel camera with 440 photomultipliers.

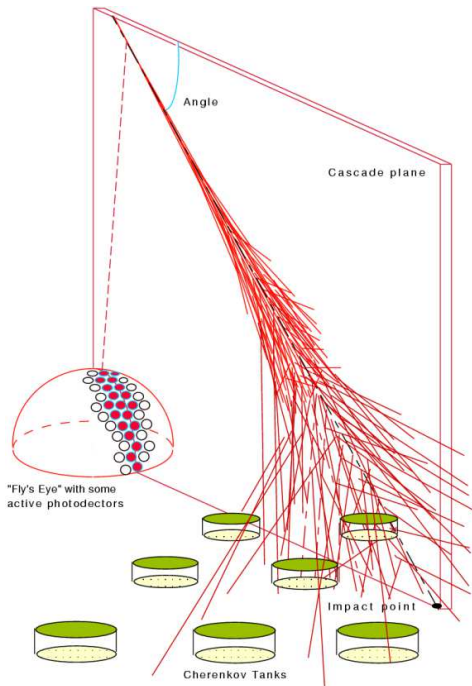


Figure 4. A cartoon of the hybrid detection technique. Charged particles at ground level are detected in SD stations while fluorescence light is collected in FD.

FD telescopes are calibrated to find the proper conversion between digitized counts and the true light flux (in photons). This calibration is performed in several steps using absolute and relative methods. The absolute calibration uses a calibrated light source (known as a 'drum') mounted at the telescope aperture [5]. Using the drum, the light flux at each pixel is known and the response is measured. In addition to the drum calibration, vertical laser

shots at wavelengths 337 and 355 nm [6, 7] are used as an independent calibration method. Between absolute calibrations (which occur several times per year), the relative response of each fluorescence camera is recorded using light pulses from LEDs and xenon flashers. The relative calibration occurs before and after each night of observations.

3.1. Hybrid Detection Technique

The two measurement techniques in use at the Pierre Auger Observatory – surface detection and air fluorescence detection – are quite complementary. (Fig. 4). Whereas SD has 100% duty cycle time and acceptance can be calculated and it is model independent, FD has duty cycle of $\approx 13\%$ [5] and acceptance depends on the atmospheric conditions (model dependent). SD measurement corresponds to one slice of a calorimeter at the last stage of shower development. To get the energy only from SD, Monte Carlo interaction models are needed in experiments without fluorescence detectors. On the other side FD collects photons emitted during development of the shower. It enables to sample a shower along its axis. Measured number of photons in different atmospheric slant depths can be converted to deposited energy to get shower longitudinal profile (Fig. 5). Then, the energy is measured directly with the atmosphere acting as a calorimeter for CR study. Events that are measured simultaneously by FD and SD are called hybrid.

Apart from the energy another very important characteristic of the shower development is the position of shower maximum. Shower maximum is the atmospheric depth where the shower longitudinal development reaches the maximum number of secondary particles.

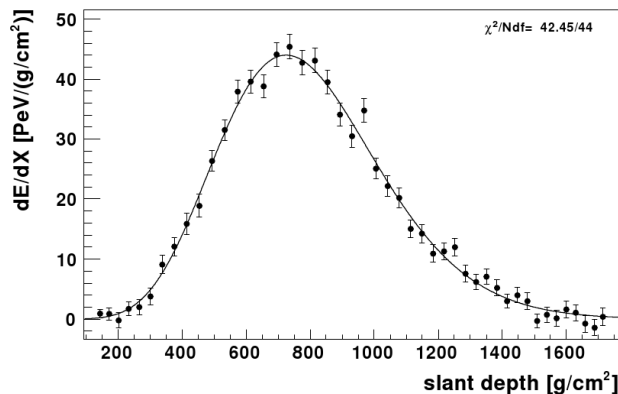


Figure 5. Longitudinal profile of energy deposit reconstructed from measured light by FD telescope. The line represents a Gaisser-Hillas function fitted to the measured profile.

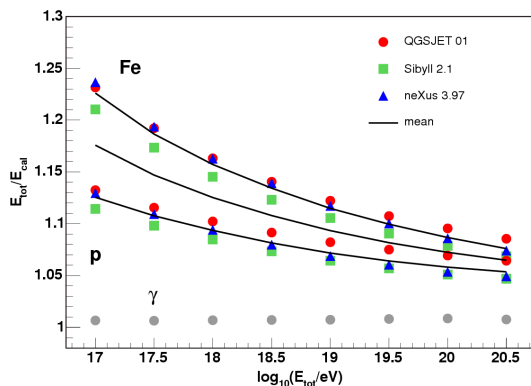


Figure 6. Correction factor for the missing energy calculated by several models (dots) with fitted curves [8] for proton and iron primaries.

3.2. FD Energy Measurement and Shower Reconstruction

Electromagnetic energy losses of charged particles are responsible for emitted fluorescence light. Therefore FD measures longitudinal shower profile. About 20 photons are emitted between 300 and 400 nm per 1 MeV loss. The total number of photons is proportional to the deposited energy of the air shower. Thus, the profile integral gives almost the whole shower energy ($\sim 90\%$ of the total energy at 10^{19} eV):

$$E_{cal} = \int dX \frac{dE}{dX}. \quad (2)$$

The remaining part ($\sim 10\%$ of the total energy at 10^{19} eV) of the shower energy cannot be directly measured by collecting emitted light. It concerns energy of neutrinos, muons and other

particles which do not excite nitrogen molecules. This type of energy is called 'missing' and it is not included in the integral of the energy deposit derived from FD data. Nevertheless, one can calculate the correction factor that depends on the primary particle type and energy (Fig 6).

3.3. SD Energy Calibration

The biggest advantage of hybrid detection is the model independent energy calibration of the SD. The energies of hybrid events are determined from FD measurement, and then the signal from the SD can be calibrated. The SD records signals from electromagnetic and muonic shower component. One shower is typically large enough to hit many SD stations. Therefore one can derive (fit) the lateral distribution function of the signal at ground. The aim of such a procedure is to find the particle signal at a distance of 1000 m from the shower core (S_{1000}). The ground parameter S_{1000} depends on the zenith angle of the primary particle. The variable corrected for the zenith angle dependency is called S_{38} and corresponds to signal S_{1000} at 38° zenith angle. The calibration is based on finding the dependency of S_{38} on the energy measured by FD (Fig. 7).

3.4. Uncertainties on the Reconstructed Energy from FD

The use of the atmosphere as a calorimeter also determines the main uncertainties of the measurement. The total systematic uncertainty in the FD energy scale is 22%, with the major contributions due to uncertainties in the fluorescence yield (14%) and atmospheric transmission (7% for aerosol scattering, 1% for Rayleigh scattering). There are also 9% uncertainties in the telescope absolute calibration, and the longitudinal shower profile reconstruction contributes 10% to the total energy uncertainty. Missing energy gives 4% uncertainty.

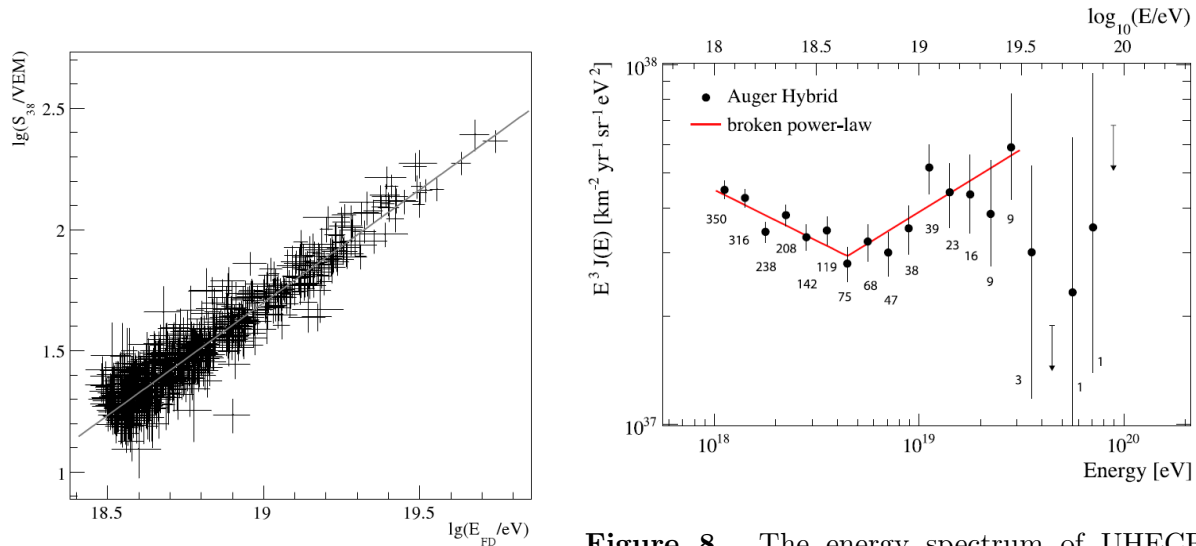


Figure 7. Ground parameter S_{38} as a function of the energy as measured with the FD for the 795 hybrid events [9].

Figure 8. The energy spectrum of UHECR determined from hybrid measurements between November 2005 and May 2008 [2]. Statistical uncertainties are shown with a broken power law used to determine the position of the ankle [2], which is clearly visible.

Several devices have been installed to monitor atmospheric conditions, especially those for optical transmission determination. For example, the Central Laser Facility [10], Lidar stations [11], and the FRAM telescope [12] are used for atmospheric monitoring program.

The measurement of the shower maximum requires a conversion of geometrical altitude as observed by FD to atmospheric depth. The conversion depends on temperature, pressure and humidity, which vary with time and location. There are meteorological stations and a balloon launch facility to measure these thermodynamical parameters. Use of measured conditions at the site considerably improves the accuracy of the air shower reconstruction [13].

The fluorescence yield is the number of photons emitted in a given band per unit of energy loss by charged particles. It is an important quantity for the energy reconstruction. The Pierre Auger Observatory uses the absolute yield from Ref. [14].

4. Conclusions

The fluorescence detector of the Pierre Auger Observatory is an atmospheric calorimeter used for the hybrid detection of air showers. It enables a model-independent energy measurement and calibration of surface detector array. The first data taking started in late 2003. The Observatory has operated steadily at its full design size since July 2008. The fluorescence detector data have enabled for example precise measurements of the UHECR energy spectrum (Fig. 8), elongation rate [15] and CR composition.

5. Acknowledgements

The contribution is prepared with the support of Ministry of Education, Youth and Sports of the Czech Republic within the project LA08016 and with the support of the Charles University in Prague within the project 119810. Special thanks to my colleagues from the Pierre Auger Collaboration for fruitful cooperation.

References

- [1] Blümer J, Engel R, Hörandel J R 2009 Cosmic rays from the knee to the highest energies *Prog. Part. Nucl. Phys.* **63** 293 (Preprint arXiv:0904.0725 [astro-ph.HE]).
- [2] Abraham J *et al.* (Pierre Auger Collaboration) 2010 Measurement of the energy of cosmic rays above 10^{18} eV using the Pierre Auger Observatory *Phys. Lett. B* **685** 239.
- [3] Abraham J *et al.* (Pierre Auger Collaboration) 2004 *Nucl. Instrum. Meth. A* **523** 50.
- [4] Abraham J *et al.* (Pierre Auger Collaboration) 2009 Operations of and Future Plans for the Pierre Auger Observatory *Proc. 31st Int. Cosmic Ray Conf. (Lodz, Poland)* (Preprint arXiv:0906.2354)
- [5] Abraham J *et al.* (Pierre Auger Collaboration) 2010 The fluorescence detector of the Pierre Auger observatory *Nucl. Instr. and Meth. in Phys. Res. A* **620** 227.
- [6] Roberts M D *et al.* (Pierre Auger Collaboration) 2003 Calibration of the Pierre Auger fluorescence detector *Proc. 28th Int. Cosmic Ray Conf. (Tsukuba, Japan)* (Preprint arXiv:astro-ph/0308410).
- [7] Knapik R *et al.* (Pierre Auger Collaboration) 2007 The absolute, relative and multi-wavelength calibration of the Pierre Auger observatory fluorescence detectors *Proc. 30th Int. Cosmic Ray Conf. (Merida, Mexico)* (Preprint arXiv:0708.1924 [astro-ph]).
- [8] Pierog T *et al.* 2005 *Proc. 29th Int. Cosmic Ray Conf. (Pune, India)* vol 7, p 103.
- [9] Giulio C *et al.* (Pierre Auger Collaboration) 2009 The cosmic ray energy spectrum and related measurements with the Pierre Auger observatory *Proc. 31st Int. Cosmic Ray Conf. (Lodz, Poland)* (Preprint arXiv:0906.2189).
- [10] Fick B *et al.* 2006 The central laser facility at the Pierre Auger observatory *JINST* **1** P11003.
- [11] BenZvi S Y *et al.* 2007 The lidar system of the Pierre Auger observatory *Nucl. Instr. Meth. A* **574** 171.
- [12] Prouza M, Jelínek M, Kubánek P, Ebr J, Trávníček P, Šmída R 2010 *Advances in Astronomy* vol 2010, Article ID 849382.
- [13] Abraham J *et al.* (Pierre Auger Collaboration) 2010 *Astropart. Phys.* **33** 108.
- [14] Nagano M *et al.* 2004 *Astropart. Phys.* **22** 235.
- [15] Abraham J *et al.* (Pierre Auger Collaboration) 2010 Measurement of the depth maximum of extensive air showers above 10^{18} eV *Phys. Rev. Letters* **104** 091101.